Salbas *et al. BMC Medical Imaging* (2025) 25:161
https://doi.org/10.1186/s12880-025-01713-1

BMC Medical Imaging

RESEARCH Open Access

Temporal evolution of MRI findings and survival outcomes in patients with brain metastases after stereotactic radiosurgery

Ali Salbas[1*], Ali Murat Koc[1], Mehmet Coskun[2], Emine Merve Horoz[3], Adem Sengul[4] and Mustafa Fazil Gelal[1]

Abstract

Objective This study aims to investigate the temporal evolution of magnetic resonance imaging (MRI) findings in brain metastases following stereotactic radiosurgery (SRS) and their correlation with treatment response and survival outcomes. By analyzing volumetric changes in tumor size, perilesional edema, and necrotic components, we seek to identify imaging biomarkers that predict prognosis and treatment efficacy.

Methods A retrospective analysis was conducted on 97 patients (200 metastatic lesions) who underwent SRS for brain metastases between 2010 and 2022. Multiparametric MRI (MPMRI) scans were analyzed at four distinct follow-up periods: 1 to 3 months, 3 to 8 months, 8 to 16 months, and 16 to 24 months post-SRS. Volumetric measurements of tumor size, perilesional edema, and necrosis were obtained using semi-automated segmentation. Apparent diffusion coefficient (ADC) values and relative cerebral blood volume (rCBV) ratios were also assessed. Statistical analyses, including Kaplan-Meier survival curves and ROC analysis, were performed to determine prognostic imaging biomarkers.

Results The most significant reduction in tumor and perilesional edema volume occurred within the first 1 to 3 months post-SRS and continued until the 8th month. A transient increase in lesion size (pseudoprogression) was observed in 31.5% of cases, predominantly between 3 and 8 months post-SRS. Pretreatment tumor volume was found to be significantly associated with treatment response. ROC analysis identified 1.22 cm^3 as the optimal cutoff value for differentiating between Group A (good response) and Group B (poor response) lesions (AUC = 0.754, sensitivity = 87.0%, specificity = 57.1%). Survival analysis revealed that higher pretreatment tumor volume, larger necrotic volume, and extensive perilesional edema were associated with shorter survival times ($p < 0.05$). No significant association was found between survival and ADC or rCBV.

Conclusion Following SRS, early reductions in tumor and edema volume were observed, while 31.5% of cases showed transient enlargement. Smaller tumors responded better to SRS, whereas larger volume, extensive edema, and necrosis were linked to shorter survival. Given the high rate of pseudoprogression, not every post-treatment size

*Correspondence:
Ali Salbas
dralisalbas@gmail.com

Full list of author information is available at the end of the article

increase indicates true progression. A wait-and-see approach may help avoid unnecessary interventions in selected cases.

Clinical trial number Not applicable.

Keywords Volumetric response, Pseudoprogression, Tumor volume, Perilesional edema, Necrosis, ADC, rCBV, Radiosurgery response, Prognostic biomarkers

Introduction

Stereotactic radiosurgery (SRS) was first introduced for the treatment of brain metastases (BMs) in the late 1980s [1, 2]. Today, SRS is widely utilized either as a standalone treatment or in combination with whole-brain radiotherapy (WBRT) for patients with BM [3]. Post-SRS follow-up magnetic resonance imaging (MRI) evaluations typically demonstrate a reduction in the size of metastatic lesions; however, transient increases in lesion size have also been reported in certain cases [4]. These enlargements observed on follow-up MR images are sometimes misinterpreted as tumor progression, leading to concerns among both clinicians and patients. However, such changes may be attributed to treatment-related inflammatory responses or radiation-induced effects.

Previous studies investigating the temporal changes in metastatic lesions following SRS have focused primarily on tumor volume alterations and treatment response. However, the evolution of perilesional edema volume after SRS and its association with clinical outcomes remain insufficiently explored. Yet, perilesional edema is a critical factor that can influence both the severity of neurological symptoms and treatment response.

In this retrospective study, we aimed to evaluate the temporal changes in key radiological parameters, including tumor volume, perilesional edema volume, apparent diffusion coefficient (ADC) values, and relative cerebral blood volume (rCBV), in patients with BM who underwent serial MRI follow-ups after SRS. Additionally, by analysing the impact of these parameters on treatment response and survival, we sought to identify prognostic biomarkers for post-SRS follow-up.

Materials and methods

Study population

Local ethics committee approval was obtained for this retrospective study (2022-GOKAE-0638, 24/11/2022, No: 0541).

Patients who underwent stereotactic radiosurgery (SRS) for brain metastases at our institution's Radiation Oncology Department and subsequently underwent follow-up with multiparametric magnetic resonance imaging (MPMRI) were retrospectively reviewed.

A total of 156 patients who received SRS for cerebral metastases between 2010 and 2022 were identified. The following patients were excluded from the study:

- 27 patients who lacked pre- or post-SRS MRI or had only a single post-SRS MRI,
- 10 patients with a history of prior surgery before SRS,
- 8 patients who had undergone whole-brain radiotherapy (WBRT) either before SRS or during follow-up,
- 2 patients who developed major intralesional hemorrhage during follow-up,
- 7 patients whose imaging data lacked contrast-enhanced high-resolution T1-weighted (T1W) and T2-weighted/FLAIR sequences.
- Five patients who received more than one SRS treatment course for the same lesion within the 24-month follow-up period were excluded.

Note However, lesions treated with multi-fraction SRS in a single course and patients who received additional SRS for newly developed lesions during follow-up were not excluded.

As a result, a final study group consisting of 97 patients and 200 metastatic lesions was established. The inclusion and exclusion criteria are summarized in Fig. 1.

Age, sex, primary tumor histology, survival time, number and location of lesions, SRS dose, and receipt of concomitant chemotherapy were recorded. All patients underwent follow-up with multiparametric magnetic resonance imaging (MPMRI) for 24 months. Owing to variations in the clinical course, the frequency of imaging varied among patients, with follow-up scans performed between the 1st and 24th months after SRS.

Based on post-treatment time intervals, patients were categorized into four groups: 1 to 3 months, 3 to 8 months, 8 to 16 months, and 16 to 24 months. MRI scans obtained during these timeframes were analyzed and evaluated.

Stereotactic radiosurgery protocol

All SRS procedures were performed using the CyberKnife Robotic Radiosurgery System (Accuray Inc., Sunnyvale, CA, USA). For treatment planning, high-resolution 3D post-contrast T1-weighted MRI and CT scans (1 mm slice thickness) were acquired with a thermoplastic mask. MRI and CT images were fused, and lesions were contoured on MRI. A 0–2 mm safety margin was added to define the planning target volume (PTV).

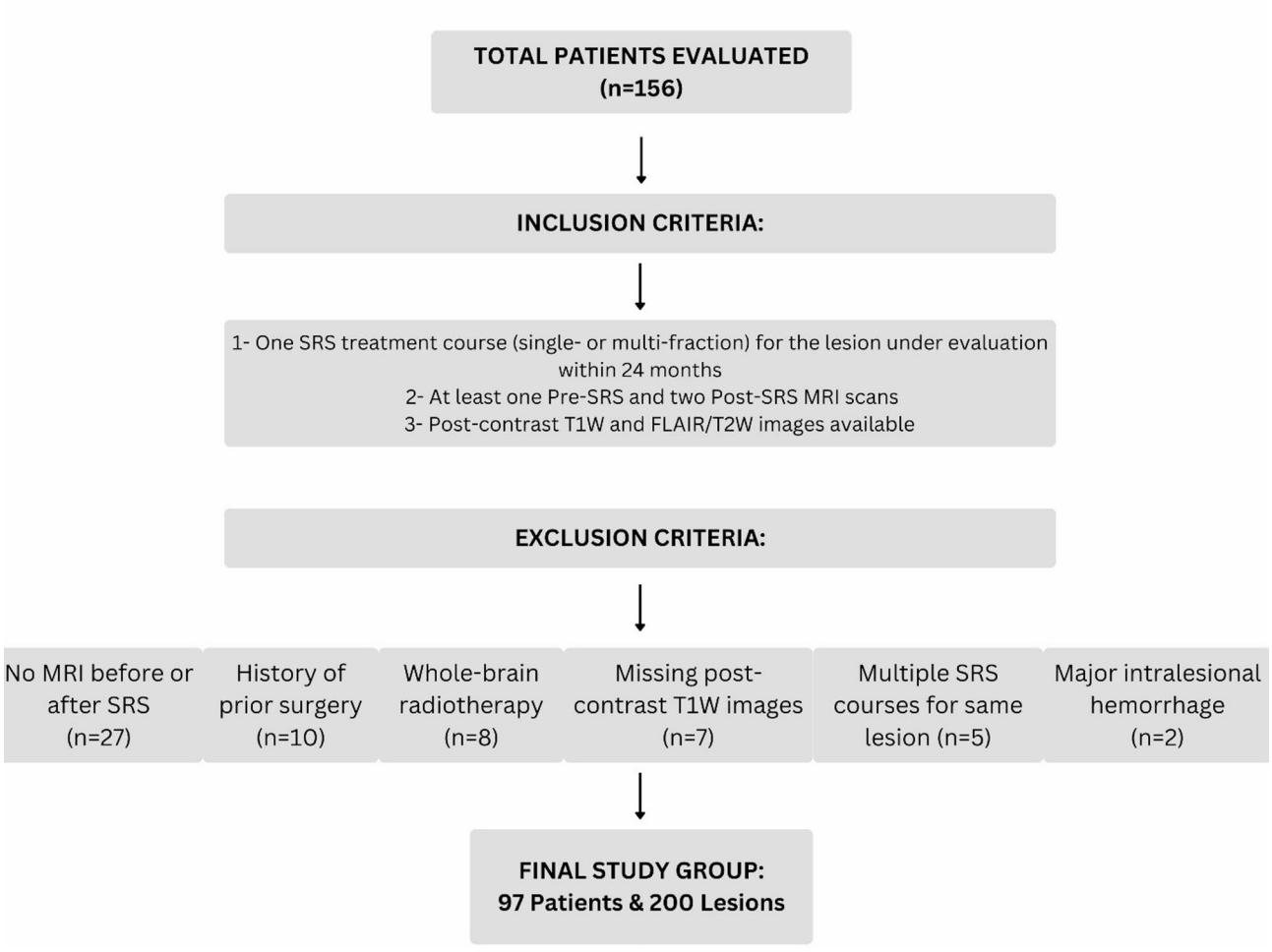

Fig. 1 Flowchart of the study enrollment population

Table 1 Siemens Magnetom 1.5 Tesla MRI sequence parameters

Parameter	T2W	T2 FLAIR	DWI	Contrast-Enhanced T1W	T2* (DSC Perfusion)
TE (ms)	99	86	60	4,86	30
TR (ms)	4000	8000	4800	13	3040
TI (ms)		2371		-	-
Slice Thickness (mm)	5	5	5	1	3
Slice Gap (mm)	1.5	1.5	1.5	1.5	3.9
Field of View (FOV) (mm)	230	230	230	230	220
b-value (s/mm^2)	-	-	1000	-	-

To minimize the risk of acute peritumoral edema, all patients received 8 mg of dexamethasone and a proton pump inhibitor on the day of treatment. Additionally, ongoing systemic therapies—such as chemotherapy, targeted therapy, or immunotherapy—were temporarily withheld and not administered concurrently with SRS, in order to reduce potential interactions and treatment-related complications.

Table 2 GE Optima 360 1.5 Tesla MRI sequence parameters

Parameter	T2W	T2 FLAIR	DWI	Contrast-Enhanced T1W
TE (ms)	84	122	103.1	3.9
TR (ms)	4222	9000	5656	10
TI (ms)	-	2200	-	-
Slice Thickness (mm)	5.5	5.5	5.5	1.4
Slice Gap (mm)	1.6	1.6	1.6	1.6
Field of View (FOV) (mm)	220	220	220	256
b-value (s/mm^2)	-	-	1000	-

Magnetic resonance imaging acquisition

All imaging was performed using 1.5 Tesla MRI scanners (Magnetom, Siemens Healthcare, Erlangen, Germany; Optima 360, GE, Fairfield, USA) using a 32-channel head coil while patients were in the supine position. The imaging parameters for each scanner are detailed in Tables 1 and 2. Sequence parameters were predefined and could not be modified by the operators.

Images were acquired following the administration of a 0.1 mmol/kg gadolinium (Gd)-based contrast agent.

Perfusion imaging was performed using the dynamic susceptibility contrast (DSC) perfusion method, which was available only on the first scanner (Table 1).

Approximately half of the total contrast dose was administered as a saturation dose, followed by a 5-minute delay before injecting the remaining contrast agent using an infusion pump at a rate no slower than 5 mL/min. This was followed by the injection of 20–25 mL of physiological saline.

MRI acquisition was initiated in cine mode, and contrast injection was performed 20 s after the sequence started, with images obtained using GRE-EPI T2* sequences with a temporal resolution of 2 s.

Multiparametric MRI analysis and image evaluation

Pre- and post-SRS follow-up images were evaluated by two radiologists with 5 and 7 years of experience, respectively, using T2W-FLAIR, ADC maps, postcontrast 3D T1-weighted images, and DSC perfusion data (rCBV maps). Both radiologists independently assessed the images and aimed to reach a consensus on the findings.

In cases of disagreement, a third expert with 27 years of experience in neuroradiology was consulted, and the final decision was made under their guidance. During the evaluation process, the radiologists were blinded to the clinical data and treatment responses of the patients to ensure unbiased analysis.

Volumetric analysis

The volumes of the solid and necrotic components of the lesions were measured using postcontrast high-resolution 3D T1-weighted images, while perilesional edema volume was assessed on T2W and FLAIR images. A freeware software program, 3D Slicer, was used for these measurements [5].

After removing demographic data and anonymizing the cases, the images were converted to Digital Imaging and Communications in Medicine (DICOM) format and imported into the software. The regions designated for volumetric measurement were semi-automatically segmented using the "Editor" module within the software, followed by manual corrections, which were then saved (Fig. 2). Manual corrections were jointly reviewed by the same two radiologists (5 and 7 years of experience) as described above, and in case of disagreement, consensus was reached with the guidance of the senior expert neuroradiologist (27 years of experience).

ADC (Apparent Diffusion Coefficient) measurements

Quantitative ADC measurements were performed using Syngo.via (Serial No: 221348, Siemens Healthineers, Erlangen, Germany) and Advantage Windows Workstation (Version 4.5, GE Healthcare Technology, Fairfield, USA). To avoid cystic-necrotic components, quantitative measurements were obtained by manually drawing freehand regions of interest (ROIs) in three separate areas showing the most prominent diffusion restriction on visual assessment. The mean ADC value was calculated by averaging these three measurements. The size and morphology of the tumor influenced the selection of ROIs, which ranged from 5 to 10 mm^2 (Fig. 2). Due to extremely small lesion sizes, ADC measurements could not be performed for 18 lesions (9%).

Perfusion MRI analysis (rCBV maps)

rCBV (relative cerebral blood volume) maps were generated and analysed using the Syngo.via workstation (Siemens Healthineers). To avoid necrotic areas and vascular structures, rCBV measurements were obtained from the most hyperperfused regions of the solid lesion and the normal-appearing white matter in the contralateral hemisphere on the same slice. To minimize bias, three ROIs were placed within each lesion, and rCBV was measured using the freehand technique. The mean rCBV value was calculated by averaging these three measurements. If no perfused region was identified within a lesion, measurements were taken from the non-perfused solid portion of the lesion. The tumor's size and morphology influenced ROI selection, with dimensions ranging from 5 to 10 mm^2. The rCBV was calculated by dividing the tumor rCBV by the rCBV of the contralateral normal-appearing white matter (Fig. 2).

Lesion classification based on volumetric changes

Lesions were categorized into four groups based on volumetric changes observed during follow-up. The classification was adapted from the RANO-BM criteria [6]:

- Group A (Good Response to Treatment):
  - Lesions that showed a ≥ 30% reduction in tumor volume and never exhibited volume increase.
- Group B (Poor Response to Treatment – No Response):
  - Lesions that demonstrated a ≥ 20% increase in tumor volume and never showed volumetric reduction.
- Group C (Pseudoprogression):
  - Lesions that initially increased in volume after treatment but subsequently shrank during follow-up.
- Group D (Progression After Temporary Response):

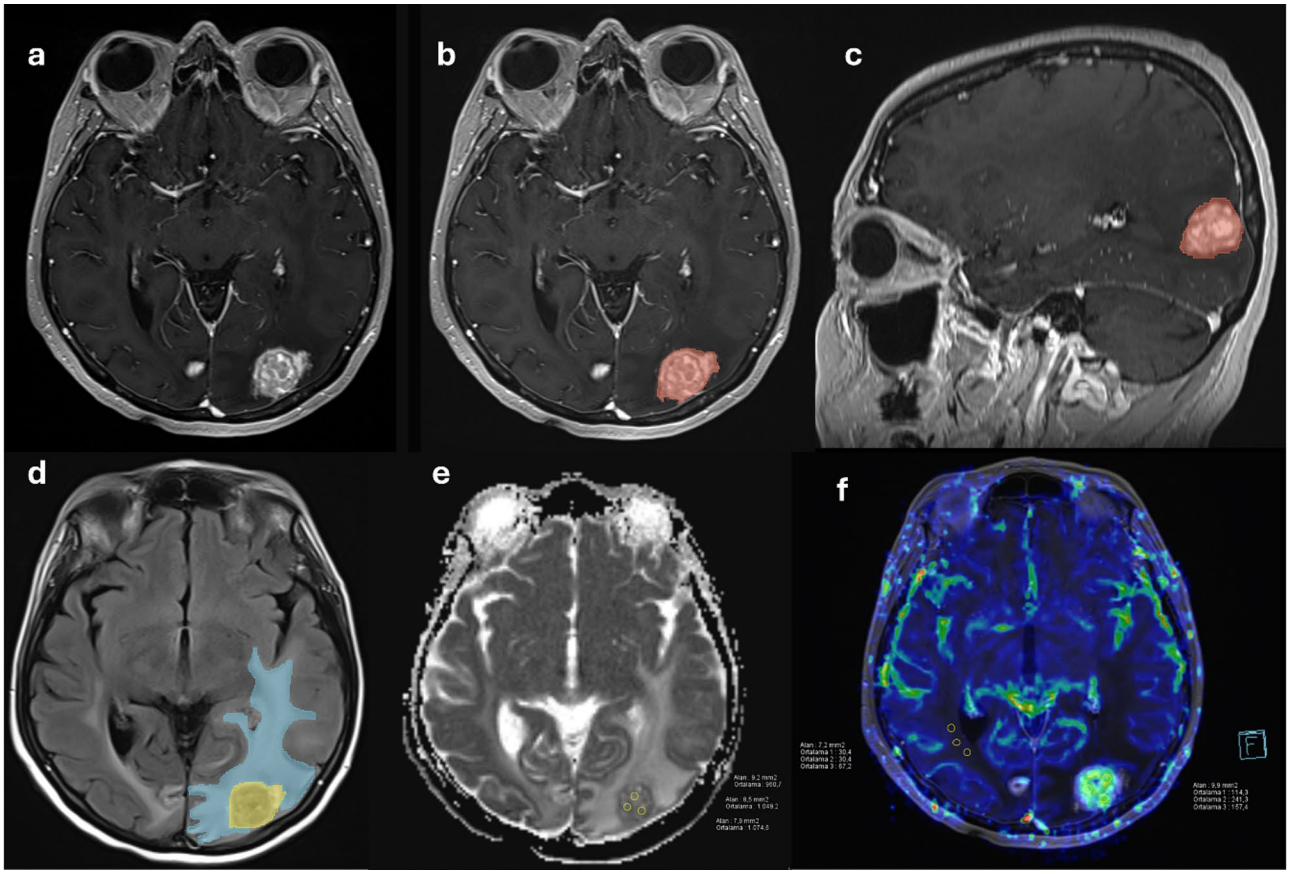

Fig. 2 (**a**) Pre-SRS imaging in a case with brain metastases from breast cancer shows the contrast-enhanced T1-weighted 3D image of the tumor. (**b**, **c**) Semi-automatic segmentation of the tumor in axial and sagittal views. (**d**) Semi-automatic segmentation of perilesional edema on axial FLAIR images. (**e**, **f**) ADC and perfusion images demonstrating ADC and rCBV measurements

– Lesions that initially decreased in volume after treatment but later exhibited progression during follow-up.

The relationships between these four groups and pretreatment demographic data, as well as MRI findings, were analysed.

Statistical analysis

Nonparametric comparisons of more than two dependent numerical variables were performed using the Friedman test. Pairwise comparisons between time points (within the same lesion) were conducted using the Wilcoxon signed-rank test with Bonferroni correction.

Categorical variables were analyzed using the Pearson chi-square test. Comparisons of three or more independent groups were performed using the Kruskal-Wallis test, and pairwise comparisons between independent groups were conducted using the Mann-Whitney U test with Bonferroni correction.

Receiver operating characteristic (ROC) analysis was used to assess the ability of pretreatment lesion volume to differentiate between response groups (Groups A and B), and to calculate the optimal cutoff value, sensitivity, specificity, and area under the curve (AUC).

Survival analysis was performed using the Kaplan–Meier method, and survival curves were compared using the log-rank test. For survival analysis, the time interval was calculated from the date of SRS to either the date of death (for deceased patients) or the last follow-up date (for censored cases).

All statistical analyses were conducted using IBM® SPSS© version 25. A p-value of < 0.05 was considered statistically significant.

Results

Demographic and clinical characteristics

A total of 62 patients (63.9%) were female, while 35 patients (36.1%) were male. The overall median age was 57 years (range: 34–85), with a median age of 55 years (range: 34–85) in females and 64 years (range: 52–82) in males. Among the 200 treated lesions, the median prescribed radiation dose was 20 Gy (IQR: 18–24 Gy), and the median number of fractions was 1 (IQR: 1–3). A total of 142 lesions (71.0%) received single-fraction stereotactic radiosurgery (SRS), while the remaining 58 lesions

Table 3 Demographic and clinical characteristics of the study population

Demographic and clinical characteristics		*N* (Number of Patients)	% (Percentage)
Gender	Female	62	63.9
	Male	35	36.1
Chemotherapy	Present	89	81.4
	Absent	8	18.6
Cancer Type	Lung	50	51.5
	Breast	37	38.1
	Ovary	5	5.2
	Others (Gastrointestinal System, Parotid, Malignant Melanoma, Squamous Cell Carcinoma)	5	5.2
Tumor Location	Supratentorial	131	65.5
	Infratentorial	69	34.5
Total Number of Lesions	1	33	34
	2	28	28.9
	3	12	12.4
	≥ 4	24	24.7
Number of Post-Treatment MRIs	2	33	34
	3	36	37.2
	≥ 4	28	28.8
Pretreatment Tumor Volume	≤ 1 cm^3	133	66.5
	1–2 cm^3	24	12
	2–4 cm^3	22	12
	≥ 4 cm^3	21	10.5

(29.0%) were treated with multi-fraction SRS protocols. The median follow-up duration was 12 months (range: 3–24). During the follow-up period, 74 patients (76.3%) had died.

Lesion characteristics

A total of 200 metastatic lesions were included in the study. Approximately two-thirds (66.5%, $n = 133$) of the lesions were smaller than 1 cm^3, while 24 lesions (12%) measured between 1 and 2 cm^3, 22 lesions (11%) ranged from 2 to 4 cm^3, and 21 lesions (10.5%) were larger than 4 cm^3 (Table 3).

Temporal changes in radiological findings

Radiological findings were evaluated at five distinct time intervals, including pre-SRS, 1 to 3 months, 3 to 8 months, 8 to 16 months, and 16 to 24 months post-SRS, and comparisons among these groups were conducted. The numbers of patients and lesions with available imaging data at each follow-up interval were as follows: baseline (97 patients, 200 lesions), 1–3 months (92 patients, 182 lesions), 3–8 months (94 patients, 194 lesions), 8–16 months (62 patients, 133 lesions), and 16–24 months (35 patients, 94 lesions). The median values and ranges of the measurements are presented in Table 4.

A statistically significant difference was found among the groups when comparing the five tumor volume measurements ($p < 0.001$). In pairwise comparisons, the pretreatment tumor volume was significantly larger than the volumes at 1 to 3 months, 3 to 8 months, and 8 to 16 months post-treatment ($p = 0.012$, $p < 0.001$, $p < 0.001$). No statistically significant differences were observed in the remaining pairwise comparisons.

A statistically significant difference was found among the groups when comparing the five perilesional edema volume measurements ($p < 0.001$). In pairwise comparisons, the pretreatment edema volume was significantly larger than the volumes at 1 to 3 months, 3 to 8 months, 8 to 16 months, and 16 to 24 months post-treatment ($p < 0.001$, $p < 0.001$, $p = 0.001$, $p = 0.014$). No statistically significant differences were observed in the remaining pairwise comparisons.

The necrosis volume, ADC value, and CBV ratio across the five time intervals were compared, and no statistically significant differences were found ($p = 0.134$, $p = 0.223$, $p = 0.459$).

When evaluating temporal changes in the lesions, tumor volume decreased by approximately 45.8% within the first 1 to 3 months after SRS, with the most significant reduction observed during this period. The decline in tumor volume continued until the 8th month, after which it began to increase again (Fig. 3).

Similarly, the greatest reduction in perilesional edema volume was observed during the 1 to 3-month period post-SRS. The edema volume continued to decrease, following a pattern similar to tumor volume reduction, until the 8th month (Fig. 3).

Table 4 Median values and ranges of tumor volume, edema volume, necrosis volume, ADC, and rCBV ratio measurements before and after SRS across Follow-up intervals

Measurement	Pre-Treatment	1–3 months	3–8 months	8–16 months	16–24 months
***Tumor Volume (cm^3)**	0.351 (0.01–35.86)	0.19 (0.02–8.86)	0.14 (0–72.73)	0.18 (0–39.67)	0.22 (0–47.70)
***Edema Volume (cm^3)**	0.69 (0–129.29)	0.1 (0–199.42)	0 (0–275.27)	0.1 (0–142.97)	0 (0–246.58)
Necrosis Volume (cm^3)	0 (0–17.67)	0 (0–16.12)	0.001 (0–9.71)	0 (0–19.77)	0 (0–22.22)
ADC ($\mu m^2/s$)	0.85 (0.61–1.30)	0.91 (0.57–1.64)	0.91 (0.57–1.52)	0.94 (0.61–1.65)	0.95 (0.52–1.82)
rCBV Ratio	2.22 (0.76–13.14)	1.66 (0.71–5.51)	1.24 (0.15–5.68)	1.53 (0.5–22)	1.42 (0.32–25.5)

* Statistically significant differences were observed in pairwise comparisons ($p < 0.05$)

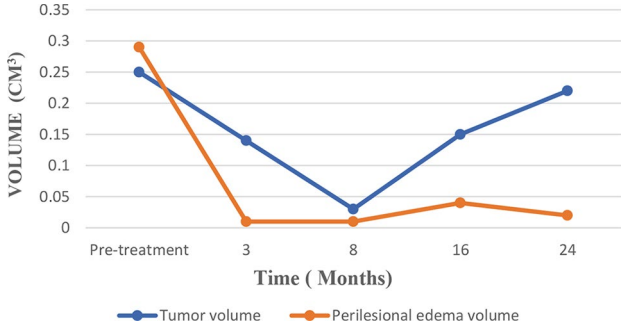

Fig. 3 Temporal changes in median tumor volume and perilesional edema volume. Number of lesions analyzed at each time point: baseline ($n=200$), 1–3 months ($n=182$), 3–8 months ($n=194$), 8–16 months ($n=133$), 16–24 months ($n=94$)

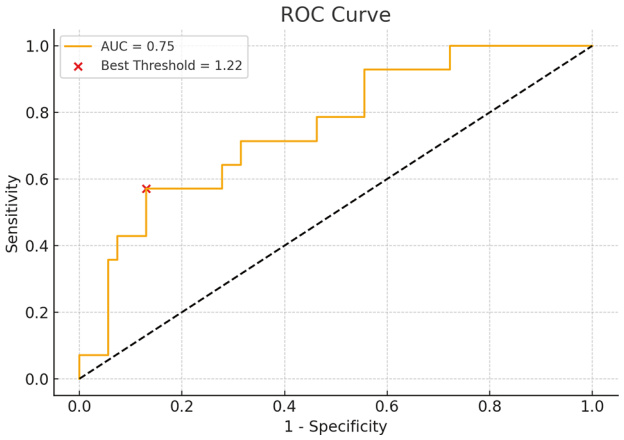

Fig. 5 ROC analysis of pre-treatment tumor volume for differentiating Group A and Group B lesions

Classification of lesions based on treatment response and volumetric changes

Lesions were classified into four groups based on volumetric changes observed during follow-up (Fig. 4).

When the four lesion groups were compared in terms of age, sex, primary tumor histology, lesion location, SRS dose, ADC value, and rCBV, no statistically significant differences were found ($p>0.05$). However, a significant difference was observed in pretreatment tumor volume among the groups ($p=0.004$). In pairwise comparisons, the pretreatment tumor volume of Group A lesions was significantly smaller than that of Group D and Group B lesions ($p=0.019$).

ROC analysis was performed to differentiate Group A and Group B lesions based on their pretreatment tumor volumes, yielding a cutoff value of 1.22 cm^3 with a sensitivity of 87.0% and specificity of 57.1% (AUC = 0.754, $p=0.004$, 95% CI: 0.616–0.892) (Fig. 5).

Group C represents lesions that exhibited a transient increase in size (pseudoprogression). A transient size increase was observed in 63 out of 200 lesions (31.5%). Among these lesions, the onset of transient enlargement occurred in 13 lesions (20.7%) during the 1 to 3-month period post-SRS, 38 lesions (60.3%) during the 3 to 8-month period post-SRS, and 12 lesions (19.0%) during the 8 to 16-month period post-SRS. When these lesions were compared in terms of age, sex, primary tumor histology, lesion location, SRS dose, ADC value, and rCBV, no statistically significant differences were found ($p>0.05$).

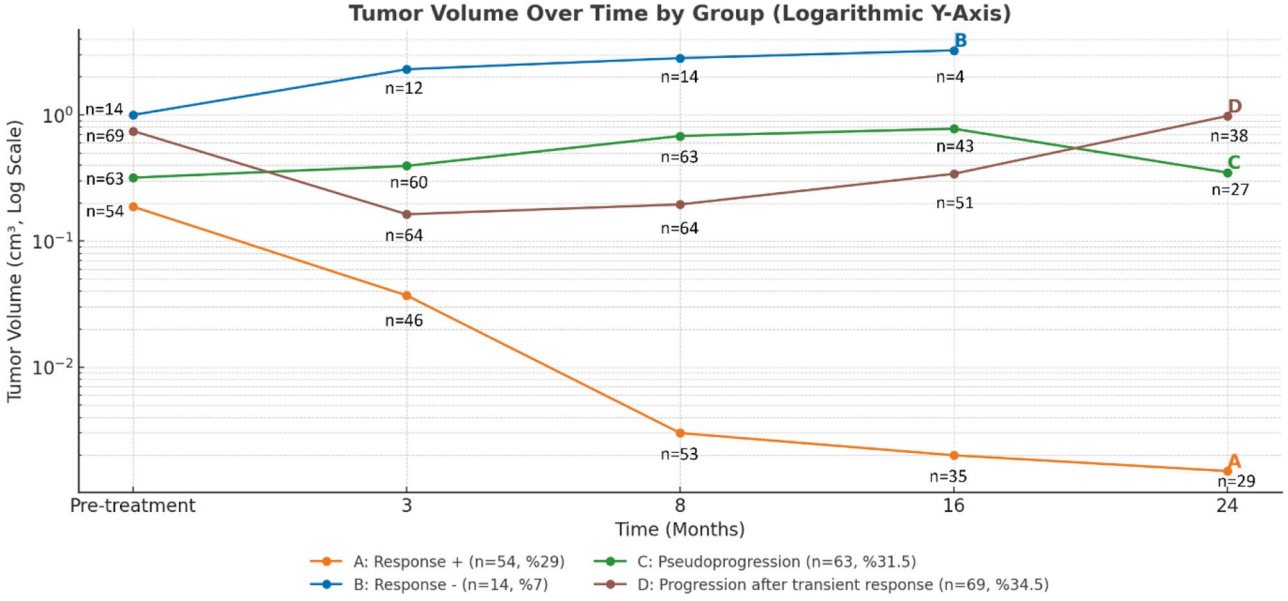

Fig. 4 Temporal evolution of tumor volume by response group (logarithmic scale). Sample sizes (n) for each group at all time points are indicated on the corresponding data points. Note: No measurable lesions remained in Group B at the final (16–24 month) time interval

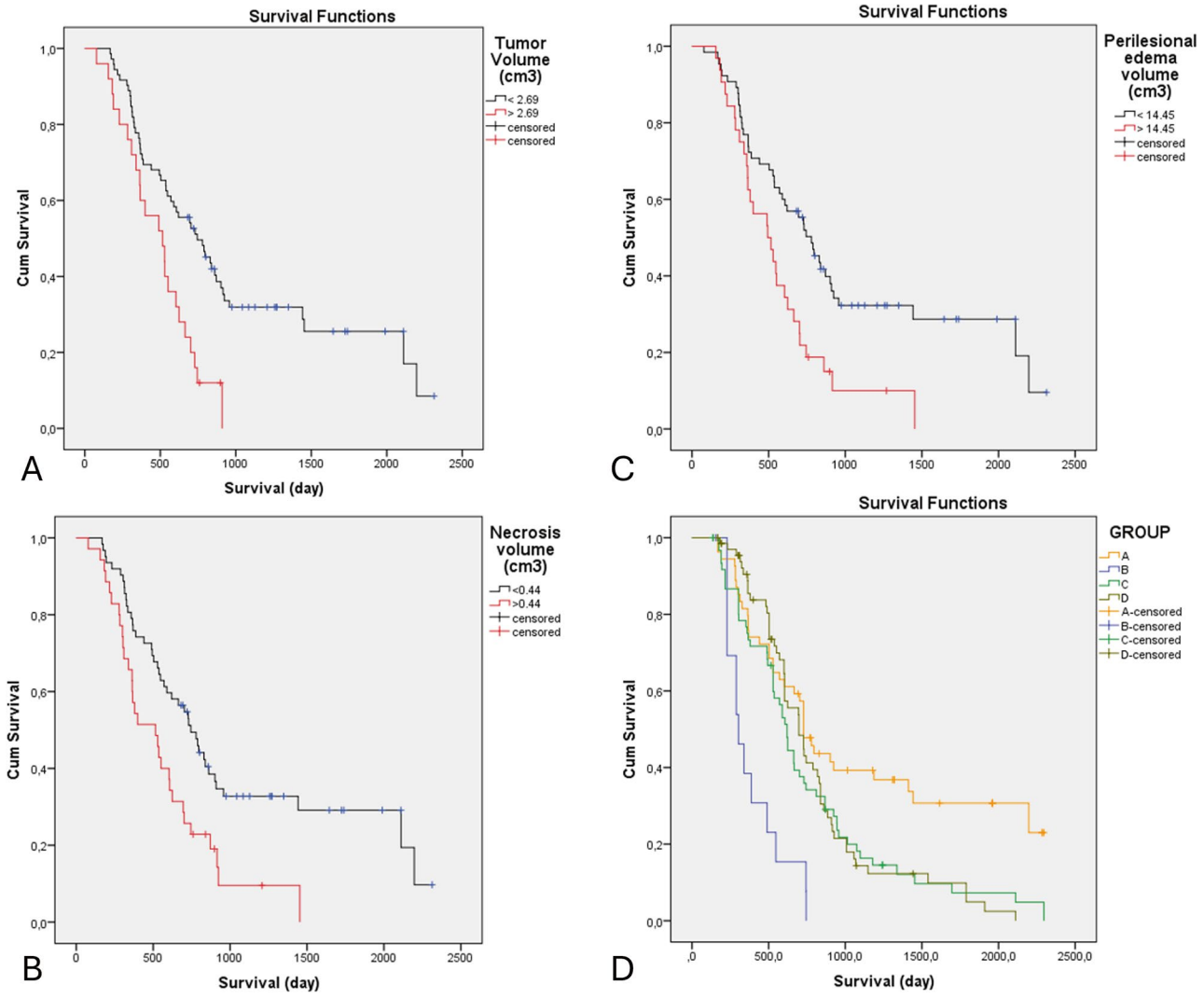

Fig. 6 Kaplan–Meier survival analyses for tumor volume (**A**), necrosis volume (**B**), perilesional edema volume (**C**), and lesion groups (**D**). Patients with larger pretreatment tumor, edema, or necrosis volumes had significantly shorter survival. Group B (poor response) showed the worst survival, while Group A (good response) had the best outcomes

Survival analysis

The median survival time of the patients was 607 days. The overall survival (OS) rates at 6, 12, and 24 months were 74%, 57%, and 31%, respectively. Survival analyses were conducted by categorizing the patients into two groups based on the mean values of different parameters.

Patients with a pretreatment tumor volume smaller than 2.69 cm^3 had a median survival of 745 days, whereas those with a tumor volume greater than 2.69 cm^3 had a median survival of 515 days, showing a statistically significant difference ($p = 0.002$). Similarly, patients with a pretreatment necrosis volume smaller than 0.44 cm^3 had a median survival of 703 days, whereas those with a necrosis volume greater than 0.44 cm^3 had a median survival of 339 days, with a statistically significant difference ($p < 0.001$).

For pretreatment perilesional edema volume, patients with a volume smaller than 14.45 cm^3 had a median survival of 728 days, while those with a volume greater than 14.45 cm^3 had a median survival of 515 days, showing a significant difference ($p = 0.028$) (Fig. 6).

No statistically significant difference was found between ADC values and survival ($p = 0.962$).

The median survival times for the lesion groups were as follows: 728 days for Group A, 303 days for Group B, 620 days for Group C, and 697 days for Group D. Survival in Group B was significantly lower than that in the other three groups ($p = 0.031$), whereas survival in Group A was significantly higher than that in the other three groups ($p = 0.028$) (Fig. 6).

Discussion

This study investigated not only the radiological evolution of brain metastases following stereotactic radiosurgery (SRS), but also imaging parameters associated with treatment response and survival.

Changes in lesion size and perilesional edema dynamics in brain metastases following stereotactic radiosurgery (SRS) are among the critical factors that directly influence clinical decision-making. In a study evaluating 100 brain metastases after SRS, Sharpton et al. reported that the most significant volumetric reduction occurred between 6 and 12 weeks and that this reduction was associated with local tumor control [7].

Similarly, several studies have reported that the most pronounced volume reduction occurs within the first 1 to 3 months [4, 8]. Our findings are consistent with these data, as the most striking changes were observed during the 1 to 3-month and 3 to 8-month intervals. Notably, the most significant tumor volume regression was observed within the first 1 to 3 months, and although this trend gradually diminished, it continued until the 8th month.

The literature indicates that the mechanisms of edema formation differ between metastatic and primary brain tumors, with metastases lacking significant tumor cell infiltration into the surrounding brain tissue, unlike glial tumors [9, 10]. Although perilesional edema in brain metastases is predominantly considered vasogenic, some studies have demonstrated the presence of neoplastic cells extending into the edematous region [11–13]. There are limited studies in the literature on the temporal changes in perilesional edema following SRS. Kaur et al. reported that perilesional edema volume decreased within the first 6 months after SRS, with the most pronounced reduction occurring in the first 3 months. Additionally, an increase in perilesional edema during the first 3 months was suggested as a potential early indicator of tumor progression [14]. Our study also demonstrated that the most significant reduction in perilesional edema occurred during the 1 to 3-month period post-SRS, following a pattern similar to tumor volume reduction, and continued until the 8th month. We believe that the reduction in peritumoral edema after SRS is directly related to tumor volume shrinkage.

Previous studies have suggested that perilesional edema may inversely correlate with $CD8^+$ tumor-infiltrating lymphocytes (TILs), and that radiation therapy may enhance antitumor immunity through modulation of the tumor microenvironment [15, 16]. Therefore, the reduction in peritumoral edema following SRS may, at least in part, be mediated by radiation-induced immunomodulatory mechanisms.

It is well known that conventional tumor ADC values are inversely correlated with tumor cellularity [17]. The literature reports that a significant increase in ADC values is observed following SRS and that this increase may serve as a potential biomarker for treatment response [18–20]. Additionally, ADC elevation has been suggested as a useful parameter in distinguishing pseudoprogression from true progression. Although an increase in ADC values was observed after SRS in our study, no statistically significant difference was detected compared to pretreatment values. The small pretreatment volumes of most lesions and the inherent limitations in measurement precision may have influenced this outcome.

A decrease in rCBV compared to pre-treatment levels has been reported in both brain metastases and glial tumors following stereotactic radiotherapy [21, 22]. In our study, although rCBV showed a decreasing trend after SRS, no statistically significant difference was found when comparing pretreatment and post-SRS rCBV values. Perfusion MRI was available for 42 patients, and this finding may be attributed to the limited number of patients included in the perfusion analysis.

In our study, transient lesion enlargement was observed in 63 lesions (31.5%). This increase typically began during the 1 to 3-month period and persisted until the 16th month in some lesions.In a study by Patel et al., which evaluated 500 brain metastases treated with SRS, transient lesion enlargement was observed in approximately one-third of the lesions, beginning as early as the 6th week post-treatment and continuing up to the 15th month [4]. Similarly, another study reported transient enlargement in approximately 28% of lesions [23]. This transient lesion enlargement, as demonstrated in these studies, is thought to be associated with radiation-induced inflammation and necrosis processes. In our study, no significant association was identified between transient enlargement and any specific factor. However, previous studies have suggested that higher radiation doses, cancer type, and male sex may be associated with transient lesion enlargement [4, 24]. In addition to early treatment responses, we observed different temporal response patterns during follow-up, including transient enlargement and delayed progression. These findings highlight that a simple increase in lesion volume—particularly in the absence of other clinical or radiological signs—should be interpreted with caution. Recognizing the diversity of volumetric response patterns may support more individualized decision-making in the follow-up management of brain metastases after SRS.

Conflicting results have been reported in the literature regarding the effectiveness of SRS in large tumors. Some studies suggest that SRS success decreases in lesions larger than 3 cm^3, leading to lower local response rates [25]. In contrast, other studies have shown that SRS is well tolerated in large metastatic lesions, with low neurotoxicity and effective tumor volume reduction [26, 27]. In our study, smaller-volume lesions exhibited a

better response to SRS treatment, whereas larger lesions showed a more limited response. We believe that smaller lesions respond more favorably due to factors such as better tissue perfusion and a more effective radiobiological response. Conversely, the limited presence of these factors in larger lesions may contribute to reduced treatment efficacy.

Numerous studies in the literature have reported an inverse relationship between tumor volume and local control. Cutoff values of 1 cm^3 and 2 cm^3 are commonly cited in these studies [28–30]. In our study, ROC analysis performed for Group A (good treatment response) and Group B (poor treatment response) yielded a cutoff value of 1.22 cm^3. We believe that this threshold may be useful for predicting treatment response or progression. Our survival analysis, consistent with previous literature, demonstrated that larger tumor volumes are associated with poorer survival outcomes [25, 28, 31]. This finding suggests that treatment strategies should be reconsidered for patients with large-volume lesions.

There are conflicting views in the literature regarding the relationship between perilesional edema and survival in brain metastases. Spanberger et al. reported that minimal perilesional edema is associated with shorter survival times, and that these tumors exhibit more infiltrative characteristics, lower HIF1a expression, and reduced neoangiogenesis [32]. In contrast, some studies suggest that the extent of perilesional edema has no significant impact on overall survival [33]. On the other hand, increased perilesional edema has been reported to be associated with a higher risk of intracranial progression, reduced response to radiotherapy, and shorter survival times in patients with metastatic lung cancer [34]. Similarly, some studies on primary brain tumors have suggested that greater perilesional edema is linked to poorer survival outcomes, which may be explained by tumor cell infiltration into peritumoral edema regions [35, 36]. Our findings are consistent with the literature, as we observed that patients with higher edema volumes had shorter survival times. We consider that this may be related to increased tumor aggressiveness and a diminished response to SRS. Perilesional edema should not be regarded merely as a side effect, but rather as a reflection of tumor biology and aggressiveness. Future studies should focus on the potential use of perilesional edema as a biomarker and further investigate edema dynamics in larger patient cohorts.

In our study, the volume of the necrotic component within the lesions was measured. Existing studies in the literature primarily focus on radiation necrosis, whereas our study specifically evaluated the pretreatment necrotic component of the tumor that did not exhibit contrast enhancement. The relationship between pretreatment necrotic components and survival in brain metastases has been relatively less investigated in the literature. In a study by Yoo et al., metastases with a higher necrotic content were associated with shorter survival, and the increase in tumor volume paralleled the increase in necrotic component volume [37]. Similarly, another study reported an inverse relationship between pre-treatment necrotic volume and survival [38].

In our study, patients with a pre-SRS necrotic component volume greater than 0.44 cm^3 exhibited shorter survival times. As tumor volume increases, the proportion of necrotic components also rises, potentially contributing to more aggressive tumor behavior through mechanisms such as hypoxia and inflammation. Our findings suggest that the necrotic component of the tumor may serve as a significant prognostic marker for survival.

This study has several limitations. First, its retrospective, single-center design and modest sample size may limit generalizability. Second, follow-up MRI intervals were not fully standardized, and the decreasing number of evaluable lesions over time may have impacted consistency. Third, the use of 5–5.5 mm slice thickness in FLAIR and T2-weighted sequences for perilesional edema assessment may have introduced partial volume effects. In addition, since RANO-BM criteria are based on percentage volume change, response classification may have been affected in lesions with different initial sizes. Moreover, additional treatments received during follow-up were not systematically documented, and causes of death were not always accessible. Finally, clinical outcomes such as neurological function or quality of life were not evaluated. Future studies with larger cohorts, standardized imaging protocols, and longitudinal clinical data are warranted to validate and expand upon these findings. Despite these limitations, our study highlights key radiological parameters that may help guide post-SRS monitoring and clinical decision-making.

Conclusion

Our study highlights the temporal dynamics of radiological changes following SRS for brain metastases. The most notable reductions in tumor and perilesional edema volumes occurred within the first 1–3 months post-treatment. Larger tumor volumes were linked to poorer survival, with a 1.22 cm^3 pretreatment threshold identified as a potential predictor of response. Beyond these general trends, distinct temporal response patterns such as transient enlargement (pseudoprogression) and delayed progression were also identified. Notably, isolated volumetric increases on follow-up imaging do not always indicate true tumor progression; therefore, a wait-and-see approach may be beneficial in selected cases. Overall, a detailed assessment of radiological parameters and awareness of atypical post-SRS response patterns may contribute to improved patient management.

Abbreviations

ADC	Apparent Diffusion Coefficient
AUC	Area Under the Curve
BM	Brain Metastases
CBV	Cerebral Blood Volume
CI	Confidence Interval
DSC	Dynamic Susceptibility Contrast
DWI	Diffusion–Weighted Imaging
FLAIR	Fluid–Attenuated Inversion Recovery
FOV	Field of View
Gd	Gadolinium
GRE	Gradient Echo
HIF1a	Hypoxia–Inducible Factor 1–alpha
MPMRI	Multiparametric Magnetic Resonance Imaging
MRI	Magnetic Resonance Imaging
rCBV	Relative Cerebral Blood Volume
ROI	Region of Interest
ROC	Receiver Operating Characteristic
SRS	Stereotactic Radiosurgery
T1W	T1–Weighted Imaging
T2W	T2–Weighted Imaging
TE	Echo Time
TI	Inversion Time
TR	Repetition Time
WBRT	Whole Brain Radiotherapy

Acknowledgements
Not applicable.

Author contributions
All authors have reviewed and approved the submitted manuscript for publication. AS was the project administrator and organized the data curation, measurements, design, literature review, and writing of the manuscript. AMK contributed to the literature review and design of the study. EMH contributed to data collection, measurements, and analysis. AdS and MC reviewed the draft, and MFG contributed to the formal analysis and literature review of the study, draft review, and editing of the manuscript. The authors agree to be accountable for all aspects of the work, ensuring integrity and accuracy.

Funding
No funding was received for conducting this study.

Data availability
The datasets used and/or analyzed during the current study are available from the corresponding author on reasonable request.

Declarations

Ethics approval and consent to participate
This retrospective study was approved by the Institutional Ethics Committee (Non-Invasive Clinical Research Ethics Committee of Izmir Katip Celebi University, application number 2022-GOKAE-0638, dated 22/11/2022, Decision no: 0541) and was conducted in accordance with the 1964 Helsinki Declaration and its later amendments or comparable ethical standards. The ethics committee (Non-Invasive Clinical Research Ethics Committee of Izmir Katip Celebi University) waived informed consent due to the retrospective nature of the study.

Consent for publication
Not applicable.

Competing interests
The authors declare no competing interests.

Author details
[1]Department of Radiology, Ataturk Training and Research Hospital, Izmir Katip Celebi University, Izmir 35150, Turkey
[2]Department of Radiology, University of Health Science Dr. Behcet Uz Children Disease and Surgery Training and Research Hospital, Izmir 35100, Turkey
[3]Department of Radiology, Izmir Democracy University, Izmir 35140, Turkey
[4]Department of Radiation Oncology, Ataturk Training and Research Hospital, Izmir Katip Celebi University, Izmir 35150, Turkey

Received: 5 March 2025 / Accepted: 6 May 2025
Published online: 14 May 2025

References

1. Lunsford LD, Flickinger J, Lindner G, Maitz A. Stereotactic Radiosurgery of the Brain Using the First United States 201 Cobalt-60 Source Gamma Knife. Neurosurgery [Internet]. 1989;24(2):151–9. Available from: http://journals.lww.com/00006123-198902000-00001
2. Nieder C, Grosu AL, Gaspar LE. Stereotactic radiosurgery (SRS) for brain metastases: A systematic review. Radiation Oncology. BioMed Central Ltd. 2014;9.
3. Vogelbaum MA, Brown PD, Messersmith H, Brastianos PK, Burri S, Cahill D et al. Treatment for Brain Metastases: ASCO-SNO-ASTRO Guideline. Journal of Clinical Oncology [Internet]. 2022;40(5):492–516. Available from: https://doi.org/10.1200/JCO.21.02314
4. Patel TR, McHugh BJ, Bi WL, Minja FJ, Knisely JPS, Chiang VL. A Comprehensive Review of MR Imaging Changes following Radiosurgery to 500 Brain Metastases. American Journal of Neuroradiology [Internet]. 2011;32(10):1885–92. Available from: http://www.ajnr.org/lookup/doi.org/10.3174/ajnr.A2668.
5. Fedorov A, Beichel R, Kalpathy-Cramer J, Finet J, Fillion-Robin JC, Pujol S et al. 3D Slicer as an image computing platform for the Quantitative Imaging Network. Magn Reson Imaging [Internet]. 2012;30(9):1323–41. Available from: https://linkinghub.elsevier.com/retrieve/pii/S0730725X12001816
6. Lin NU, Lee EQ, Aoyama H, Barani IJ, Barboriak DP, Baumert BG et al. Response assessment criteria for brain metastases: proposal from the RANO group. Lancet Oncol [Internet]. 2015;16(6):e270–8. Available from: https://linkinghub.elsevier.com/retrieve/pii/S1470204515700574
7. Sharpton SR, Oermann EK, Moore DT, Schreiber E, Hoffman R, Morris DE et al. The Volumetric Response of Brain Metastases After Stereotactic Radiosurgery and Its Post-treatment Implications. Neurosurgery [Internet]. 2014;74(1):9–16. Available from: https://journals.lww.com/00006123-201401000-00002
8. Oft D, Schmidt MA, Weissmann T, Roesch J, Mengling V, Masitho S et al. Volumetric Regression in Brain Metastases After Stereotactic Radiotherapy: Time Course, Predictors, and Significance. Front Oncol [Internet]. 2021;10. Available from: https://www.frontiersin.org/articles/https://doi.org/10.3389/fonc.2020.590980/full
9. Law M, Cha S, Knopp EA, Johnson G, Arnett J, Litt AW. High-Grade Gliomas and Solitary Metastases: Differentiation by Using Perfusion and Proton Spectroscopic MR Imaging. Radiology [Internet]. 2002;222(3):715–21. Available from: https://doi.org/10.1148/radiol.2223010558
10. Papadopoulos MC, Saadoun S, Binder DK, Manley GT, Krishna S, Verkman AS. Molecular mechanisms of brain tumor edema. Neuroscience [Internet]. 2004;129(4):1009–18. Available from: https://linkinghub.elsevier.com/retrieve/pii/S030645220400418X
11. Yoo H, Kim YZ, Nam BH, Shin SH, Yang HS, Lee JS et al. Reduced local recurrence of a single brain metastasis through microscopic total resection. J Neurosurg [Internet]. 2009;110(4):730–6. Available from: https://thejns.org/view/journals/j-neurosurg/110/4/article-p730.xml
12. Berghoff AS, Rajky O, Winkler F, Bartsch R, Furtner J, Hainfellner JA et al. Invasion patterns in brain metastases of solid cancers. Neuro Oncol [Internet]. 2013;15(12):1664–72. Available from: https://academic.oup.com/neuro-oncology/article-lookup/doi.org/10.1093/neuonc/not112.
13. Müller SJ, Khadhraoui E, Ernst M, Rohde V, Schatlo B, Malinova V. Differentiation of multiple brain metastases and glioblastoma with multiple foci using MRI criteria. BMC Med Imaging [Internet]. 2024;24(1):3. Available from: https://bmcmedimaging.biomedcentral.com/articles/10.1186/s12880-023-01183-3.
14. Kaur M, Cassinelli Petersen G, Jekel L, von Reppert M, Varghese S, Dixe de Oliveira Santo I et al. PACS-Integrated Tools for Peritumoral Edema Volumetrics Provide Additional Information to RANO-BM-Based Assessment of Lung Cancer Brain Metastases after Stereotactic Radiotherapy: A Pilot Study. Cancers (Basel) [Internet]. 2023;15(19):4822. Available from: https://www.mdpi.com/2072-6694/15/19/4822
15. Berghoff AS, Fuchs E, Ricken G, Mlecnik B, Bindea G, Spanberger T et al. Density of tumor-infiltrating lymphocytes correlates with extent of brain edema and overall survival time in patients with brain metastases. Oncoimmunology

[Internet]. 2015 [cited 2024 Apr 7];5(1). Available from: https://pubmed.ncbi.nlm.nih.gov/26942067/
16. Haikerwal SJ, Hagekyriakou J, MacManus M, Martin OA, Haynes NM. Building immunity to cancer with radiation therapy. Cancer Lett [Internet]. 2015;368(2):198–208. Available from: https://linkinghub.elsevier.com/retrieve/pii/S0304383515000300
17. Yamasaki F, Kurisu K, Satoh K, Arita K, Sugiyama K, Ohtaki M et al. Apparent Diffusion Coefficient of Human Brain Tumors at MR Imaging. Radiology [Internet]. 2005;235(3):985–91. Available from: https://doi.org/10.1148/radiol.2353031338
18. Tomura N, Narita K, Izumi Jichi, Suzuki A, Anbai A, Otani T et al. Diffusion Changes in a Tumor and Peritumoral Tissue After Stereotactic Irradiation for Brain Tumors. J Comput Assist Tomogr [Internet]. 2006;30(3):496–500. Available from: http://journals.lww.com/00004728-200605000-00024
19. Knitter JR, Erly WK, Stea BD, Lemole GM, Germano IM, Doshi AH et al. Interval Change in Diffusion and Perfusion MRI Parameters for the Assessment of Pseudoprogression in Cerebral Metastases Treated With Stereotactic Radiation. American Journal of Roentgenology [Internet]. 2018;211(1):168–75. Available from: https://www.ajronline.org/doi/10.2214/AJR.17.18890.
20. Huang CF, Chou HH, Tu HT, Yang MS, Lee JK, Lin LY. Diffusion magnetic resonance imaging as an evaluation of the response of brain metastases treated by stereotactic radiosurgery. Surg Neurol [Internet]. 2008;69(1):62–8. Available from: https://linkinghub.elsevier.com/retrieve/pii/S0090301907002947
21. Fuss M, Wenz F, Scholdei R, Essig M, Debus J, Knopp MV et al. Radiation-induced regional cerebral blood volume (rCBV) changes in normal brain and low-grade astrocytomas: quantification and time and dose-dependent occurrence. International Journal of Radiation Oncology*Biology*Physics [Internet]. 2000;48(1):53–8. Available from: https://linkinghub.elsevier.com/retrieve/pii/S0360301600005903
22. Kerkhof M, Ganeff I, Wiggenraad RGJ, Lycklama à Nijeholt GJ, Hammer S, Taphoorn MJB et al. Clinical applicability of and changes in perfusion MR imaging in brain metastases after stereotactic radiotherapy. J Neurooncol [Internet]. 2018;138(1):133–9. Available from: http://link.springer.com/10.1007/s11060-018-2779-7.
23. Sparacia G, Agnello F, Banco A, Bencivinni F, Anastasi A, Giordano G et al. Value of serial magnetic resonance imaging in the assessment of brain metastases volume control during stereotactic radiosurgery. World J Radiol [Internet]. 2016;8(12):916. Available from: http://www.wjgnet.com/1949-8470/full/v8/i12/916.htm
24. Kubo K, Kenjo M, Doi Y, Nakao M, Miura H, Ozawa S et al. MRI appearance change during stereotactic radiotherapy for large brain metastases and importance of treatment plan modification during treatment period. Jpn J Radiol [Internet]. 2019;37(12):850–9. Available from: http://link.springer.com/10.1007/s11604-019-00886-4
25. Ebner D, Rava P, Gorovets D, Cielo D, Hepel JT. Stereotactic radiosurgery for large brain metastases. J Clin Neurosci [Internet]. 2015 [cited 2024 Apr 7];22(10):1650–4. Available from: https://pubmed.ncbi.nlm.nih.gov/26209921/
26. Feuvret L, Vinchon S, Martin V, Lamproglou I, Halley A, Calugaru V et al. Stereotactic radiotherapy for large solitary brain metastases. Cancer Radiother [Internet]. 2014 [cited 2024 Apr 7];18(2):97–106. Available from: https://pubmed.ncbi.nlm.nih.gov/24439342/
27. Jeong WJ, Park JH, Lee EJ, Kim JH, Kim CJ, Cho YH. Efficacy and Safety of Fractionated Stereotactic Radiosurgery for Large Brain Metastases. J Korean Neurosurg Soc [Internet]. 2015 [cited 2024 Apr 7];58(3):217. Available from: http://www.pmc/articles/PMC4630352/
28. Baschnagel AM, Meyer KD, Chen PY, Krauss DJ, Olson RE, Pieper DR et al. Tumor volume as a predictor of survival and local control in patients with brain metastases treated with Gamma Knife surgery. J Neurosurg [Internet]. 2013;119(5):1139–44. Available from: https://thejns.org/view/journals/j-neurosurg/119/5/article-p1139.xml
29. Varlotto JM, Flickinger JC, Niranjan A, Bhatnagar AK, Kondziolka D, Lunsford LD. Analysis of tumor control and toxicity in patients who have survived at least one year after radiosurgery for brain metastases. International Journal of Radiation Oncology*Biology*Physics [Internet]. 2003;57(2):452–64. Available from: https://linkinghub.elsevier.com/retrieve/pii/S0360301603005686
30. Kwon AK, DiBiase SJ, Wang B, Hughes SL, Milcarek B, Zhu Y. Hypofractionated stereotactic radiotherapy for the treatment of brain metastases. Cancer [Internet]. 2009;115(4):890–8. Available from: https://acsjournals.onlinelibrary.wiley.com/doi/10.1002/cncr.24082
31. Hughes RT, Black PJ, Page BR, John T, Lucas J, Qasem SA, Watabe K et al. Local control of brain metastases after stereotactic radiosurgery: the impact of whole brain radiotherapy and treatment paradigm. J Radiosurg SBRT [Internet]. 2016 [cited 2024 Apr 7];4(2):89. Available from: http://www.pmc/articles/PMC5658880/
32. Spanberger T, Berghoff AS, Dinhof C, Ilhan-Mutlu A, Magerle M, Hutterer M et al. Extent of peritumoral brain edema correlates with prognosis, tumoral growth pattern, HIF1a expression and angiogenic activity in patients with single brain metastases. Clin Exp Metastasis [Internet]. 2013 [cited 2024 Apr 7];30(4):357–68. Available from: https://pubmed.ncbi.nlm.nih.gov/23076770/
33. Kerschbaumer J, Bauer M, Popovscaia M, Grams AE, Thomé C, Freyschlag CF. Correlation of tumor and peritumoral edema volumes with survival in patients with cerebral metastases. Anticancer Res. 2017;37(2):871–6.
34. Arrieta O, Bolaño-Guerra LM, Caballé-Pérez E, Lara-Mejía L, Turcott JG, Gutiérrez S et al. Perilesional edema diameter associated with brain metastases as a predictive factor of response to radiotherapy in non-small cell lung cancer. Front Oncol [Internet]. 2023;13. Available from: https://www.frontiersin.org/articles/10.3389/fonc.2023.1251620/full
35. Schoenegger K, Oberndorfer S, Wuschitz B, Struhal W, Hainfellner J, Prayer D et al. Peritumoral edema on MRI at initial diagnosis: an independent prognostic factor for glioblastoma? Eur J Neurol [Internet]. 2009 [cited 2024 Apr 7];16(7):874–8. Available from: https://pubmed.ncbi.nlm.nih.gov/19473360/
36. Pope WB, Sayre J, Perlina A, Villablanca JP, Mischel PS, Cloughesy TF. MR imaging correlates of survival in patients with high-grade gliomas. AJNR Am J Neuroradiol. 2005;26(10):2466–74.
37. Yoo J, Cha YJ, Park HH, Park M, Joo B, Suh SH et al. The Extent of Necrosis in Brain Metastases May Predict Subtypes of Primary Cancer and Overall Survival in Patients Receiving Craniotomy. Cancers (Basel) [Internet]. 2022 [cited 2024 Apr 6];14(7):1694. Available from: https://www.mdpi.com/2072-6694/14/7/1694.
38. Martens K, Meyners T, Rades D, Tronnier V, Bonsanto MM, Petersen D et al. The prognostic value of tumor necrosis in patients undergoing stereotactic radiosurgery of brain metastases. Radiation Oncology [Internet]. 2013;8(1):162. Available from: https://ro-journal.biomedcentral.com/articles/10.1186/1748-717X-8-162

Publisher's note